Halide-Dependent Change of the Lowest-Excited-State Character from MLCT to XLCT for the Complexes $Re(X)(CO)_3(\alpha\text{-diimine})$ (X = Cl, Br, I; α-diimine = bpy, iPr-PyCa, iPr-DAB) Studied by Resonance Raman, Time-Resolved Absorption, and Emission Spectroscopy

Brenda D. Rossenaar,[†] Derk J. Stufkens,*[,†] and Antonín Vlček, Jr.*[,‡]

Anorganisch Chemisch Laboratorium, J. H. van't Hoff Research Institute, Universiteit van Amsterdam, Nieuwe Achtergracht 166, 1018 WV Amsterdam, The Netherlands, and J. Heyrovský Institute of Physical Chemistry, Academy of Sciences of the Czech Republic, Dolejškova 3, 182 23 Prague, Czech Republic

Received July 29, 1995[⊗]

Complexes of the type $Re(X)(CO)_3(\alpha\text{-diimine})$ (X = Cl, Br, I; α-diimine = bpy, iPr-PyCa, iPr-DAB) exhibit a significant influence of X on the energies and intensities of their lowest-energy electronic transitions. Resonance Raman experiments revealed a change in character of the lowest energy transitions of these complexes from Re → α-diimine (MLCT) to X → α-diimine (XLCT) upon going from Cl to Br. This halide influence can be explained by different extents of mixing of the d_π(Re) and p_π(X) orbitals. All complexes under study are emissive at 80 K in a glass; the bpy complexes are also emissive at room temperature in fluid solution. The emission from the XLCT excited state is characterized by a longer lifetime, due to smaller k_{nr} and k_r values, than the MLCT emission. Nanosecond time-resolved absorption spectroscopy of $Re(X)(CO)_3$(bpy) revealed that the halide determines the excited state character of the complexes also in fluid solution. The transient absorption maximum shifts to lower energy going from Cl to Br to I, and the excited state lifetime increases from 50 to 57 to 79 ns, respectively. Variation of the α-diimine has less influence on the properties of the XLCT state than on those of the MLCT state.

Introduction

The spectroscopy, photophysics, and photochemistry of emissive d^6-$Re^I(L)(CO)_3(\alpha\text{-diimine})^{0/+}$ complexes continue to attract much interest[1−14] both because of emerging fundamental understanding of the nature and dynamics of electronically excited organometallic molecules and, also, for their various applications as luminophores,[15−18] photocatalysts and photosensitizers of important processes like CO_2 reduction[19−23] and solar energy conversion.[24,25] Emission of the $Re(L)(CO)_3(\alpha\text{-diimine})^{0/+}$ complexes is usually assigned to $Re^I \rightarrow \alpha$-diimine ^{3}MLCT excited state(s),[11,26−28] although emission from intraligand (^{3}IL) states (either α-diimine or L-localized) may also contribute for some ligands.[29−31] Interestingly, the excited state properties and lifetimes are strongly dependent on the nature of the axial ligand and α-diimine. Understanding of this ligand dependence is of much interest as it may be utilized either to tune deliberately the excited state properties or to employ the $Re(L)(CO)_3(\alpha\text{-diimine})^{0/+}$ complexes as substrate- or medium-specific luminescence probes whose operation is essentially based on the modification of the emission properties via interaction with the ligand(s).

Usually, the dependence of the ^{3}MLCT emission lifetimes of the $Re(L)(CO)_3(\alpha\text{-diimine})^{0/+}$ complexes on the coligand L has been explained in terms of the energy gap law.[2,13,32,33]

[†] Universiteit van Amsterdam.
[‡] Academy of Sciences of the Czech Republic.
[⊗] Abstract published in *Advance ACS Abstracts,* April 1, 1996.

(1) Balk, R. W.; Stufkens, D. J.; Oskam, A. *J. Chem. Soc., Dalton Trans.* **1981**, 1124.
(2) Caspar, J. V.; Meyer, T. J. *J. Phys. Chem.* **1983**, *87*, 952.
(3) Dominey, R. N.; Hauser, B.; Hubbard, J.; Dunham, J. *Inorg. Chem.* **1991**, *30*, 4754.
(4) George, M. W.; Johnson, F. P. A.; Westwell, J. R.; Hodges, P. M.; Turner, J. J. *J. Chem. Soc., Dalton Trans.* **1993**, 2977.
(5) Kalyanasundaram, K. *Proc. Indian Acad. Sci.* **1992**, *104*, 701.
(6) Lucia, L. A.; Burton, R. D.; Schanze, K. S. *Inorg. Chim. Acta* **1993**, *208*, 103.
(7) Reitz, G. A.; Dressich, W. J.; Demas, J. N.; DeGraff, B. A. *J. Am. Chem. Soc.* **1986**, *108*, 5344.
(8) Reitz, G. A.; Demas, J. N.; DeGraff, B. A.; Stephens, E. M. *J. Am. Chem. Soc.* **1988**, *110*, 5051.
(9) Sacksteder, L.; Lee, M.; Demas, J. N.; DeGraff, B. A. *J. Am. Chem. Soc.* **1993**, *115*, 8230.
(10) Schanze, K. S.; MacQueen, D. B.; Perkins, T. A.; Cabana, L. A. *Coord. Chem. Rev.* **1993**, *122*, 63.
(11) Smothers, W. K.; Wrighton, M. S. *J. Am. Chem. Soc.* **1983**, *105*, 1067.
(12) Striplin, D. R.; Crosby, G. A. *Chem. Phys. Lett.* **1994**, *221*, 426.
(13) Worl, L. A.; Duesing, R.; Della Ciana, L.; Meyer, T. J. *J. Chem. Soc., Dalton Trans.* **1991**, 849.
(14) Stufkens, D. J. *Comments Inorg. Chem.* **1992**, *13*, 359.
(15) Oriskovich, T. A.; White, P. S.; Thorpe, H. H. *Inorg. Chem.* **1995**, *34*, 1629.
(16) Kotch, T. G.; Lees, A. J. *Chem. Mater.* **1991**, *3*, 25.
(17) Kotch, T. G.; Lees, A. J.; Fuerniss, S. J.; Papathomas, K. I.; Snyder, R. W. *Inorg. Chem.* **1993**, *32*, 2570.
(18) Thornton, N. B.; Schanze, K. S. *Inorg. Chem.* **1993**, *32*, 4994.
(19) Ishitani, O.; George, M. W.; Ibusuki, T.; Johnson, F. P. A.; Koike, K.; Nozaki, K.; Pac, S.; Turner, J. J.; Westwell, J. R. *Inorg. Chem.* **1994**, *33*, 4712.
(20) Hawecker, J.; Lehn, J.-M.; Ziessel, R. *J. Chem. Soc., Chem. Commun.* **1983**, 536.
(21) Hawecker, J.; Lehn, J. M.; Ziessel, R. *Helv. Chim. Acta* **1986**, *69*, 1990.
(22) Calzaferri, G.; Hadener, K.; Li, J. *J. Photochem. Photobiol.* **1992**, *64*, 259.
(23) Kutal, C.; Corbin, J.; Ferraudi, G. *Organometallics* **1987**, *6*, 553.
(24) *Energy Resources through Photochemistry and Catalysis*; Grätzel, M., Ed.; Academic Press: New York, 1983.
(25) Grätzel, M. *Coord. Chem. Rev.* **1991**, *111*, 167.
(26) Wrighton, M. S.; Morse, D. L. *J. Am. Chem. Soc.* **1974**, *96*, 998.
(27) Glyn, P.; George, M. W.; Hodges, P. M.; Turner, J. J. *J. Chem. Soc., Chem. Commun.* **1989**, 1655.
(28) Lees, A. J. *Chem. Rev.* **1987**, *87*, 711.
(29) Sacksteder, L. A.; Zipp, A. P.; Brown, E. A.; Streich, J.; Demas, J. N.; DeGraff, B. A. *Inorg. Chem.* **1990**, *29*, 4335.
(30) Shaw, J. R.; Schmehl, R. H. *J. Am. Chem. Soc.* **1991**, *113*, 389.
(31) Fredericks, S. M.; Luong, J. C.; Wrighton, M. S. *J. Am. Chem. Soc.* **1979**, *101*, 7415.
(32) Englman, R.; Jortner, J. *Mol. Phys.* **1970**, *18*, 145.

S0020-1669(95)00980-3 CCC: $12.00

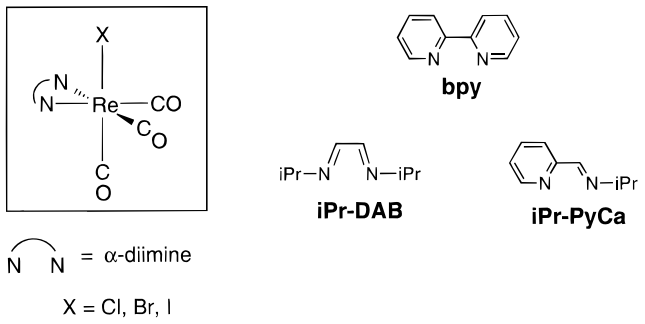

Figure 1. Molecular structures of the complexes Re(X)(CO)$_3$(α-diimine) and the α-diimine ligands used.

However, our recent spectroscopic studies on Re(X)(CO)$_3$(pTol-DAB) (X = Otf, Br)[34,35] as well as on similar d^6-Mn^I(X)(CO)$_3$(α-diimine)[36] and d^6-Ru^{II}(X)(R)(CO)$_2$(α-diimine) (X = Cl, Br, I) complexes[37−39] indicated that variation of the coligand X changes not only the energy but also the very character of the lowest (emitting) excited state. While the chloro complexes exhibit the behavior characteristic of the usual ^{3}MLCT excited state, the bromo and, especially, iodo complexes show absorption bands with different character of resonance Raman excitation profiles and, also, longer-lived emission. These spectroscopic effects have been interpreted by an increased mixing between the metal d_π and halide p_π orbitals, as the p_π orbital energy increases upon going from Cl to Br to I. For the iodo complexes, the p_π orbital might even become the HOMO. In that case, the lowest electronic transition acquires mostly an X → α-diimine XLCT (sometimes also referred to as LLCT[40,41]) character, with important consequences for the nature of the lowest excited state and, hence, for the photophysical behavior of the complex.

Surprisingly enough, the influence of the halide ligand (X = Cl, Br, I) on the excited state properties of Re(X)(CO)$_3$(α-diimine) has not yet been studied, while the investigations of the influence of the α-diimine ligand were limited only to various derivatives of bpy and phen. Should the change of the MLCT to XLCT character of the lowest excited state as a function of the ligand X occur also for the highly emissive Re(X)(CO)$_3$(α-diimine) species, it could have important implications for the understanding of the excited state dynamics of the Re(L)(CO)$_3$(α-diimine)$^{0/+}$ complexes in general, as well as for the design of new efficient luminophores and sensitizers that would absorb and/or emit light in the low-energy visible spectral region.

Hence, we have undertaken a comprehensive spectroscopic and photophysical study of Re(X)(CO)$_3$(α-diimine) (X = Cl, Br, I; α-diimine = bpy, iPr-PyCa, iPr-DAB) complexes aimed especially at the tuning of the excited state properties by ligand variations. The schematic structure of the complexes is given in Figure 1.

Experimental Section

Materials and Preparations. The complexes Re(X)(CO)$_3$(α-diimine) (X = Cl, Br, I)[42,43] were prepared from Re(X)(CO)$_5$ and the α-diimine ligand according to literature procedures. $Re_2(CO)_{10}$ was purchased from Strem and used without further purification; bpy was obtained from Merck and used as such. The solvents for spectroscopy were all of analytical grade and freshly distilled from sodium wire under N_2.

Spectroscopic Measurements and Photochemistry. All preparations for photochemical experiments were carried out under an atmosphere of purified N_2 using Schlenk techniques. The solutions were carefully handled in the dark before the experiments were performed.

Electronic absorption spectra were measured on a Varian Cary 4E or Perkin-Elmer Lambda 5 UV−vis spectrophotometer, the latter provided with a 3600 data station. Resonance Raman measurements were performed on a Dilor XY spectrometer, using an SP Model 2016 Ar ion laser as excitation source. To avoid photodecomposition during the measurements, the KNO_3 pellet containing the complex was spun. Solution Raman spectra were obtained in a spinning cell. The sample concentration was *ca.* 4×10^{-3} M.

Laser flash photolysis was used to obtain the nanosecond transient absorption spectra. The sample was excited with a Nd:YAG laser (Spectra Physics GCR-3, pulse width 7 ns (fwhm)). The desired excitation wavelength was obtained by frequency tripling of the 1064 nm 10 Hz fundamental (355 nm) or by employing a Quanta-Ray PDL-3 pulsed dye laser (Spectra Physics) with Coumarine 47 dye pumped by the 355 nm line of the Nd:YAG laser (460 nm). Typical pulse energies were 20 mJ/pulse (at 355 nm) and 14 mJ/pulse (at 460 nm). The sample concentration was such that the absorbance at the excitation wavelength was between 0.3 and 0.9 and the maximum absorbance did not exceed 1.2. A 450 W high-pressure Xe lamp pulsed with a Müller Electronik MSP05 pulser was used as probe source. After passing the sample, the probe light was transferred via a fiber to a spectrograph (EG&G Model 1234) equipped with a 150 g/mm grating and a 250 μm slit resulting in 6 nm resolution. The data collection system consisted further of a Model 1460 OMA-III console provided with a 1302 fast pulser, a 1303 gate pulser (gate = 5 ns), and a MCP-gated diode array detector (EG&G Model 1421). The transient absorption spectra at a given time delay were averaged over at least 20 laser flashes.

A similar setup, not using the flash lamp, was used for the time-resolved low-temperature emission experiments. The samples were prepared as optically dilute solutions (10^{-4}−5×10^{-3} M) of the complexes in freshly distilled solvent, which were freeze−pump−thaw degassed at least three times and subsequently sealed under vacuum. For room-temperature experiments, 1 cm quartz cuvettes (Hellma) were used. For low-temperature experiments, the glass tube of 1 cm diameter which was used as a cuvette was cooled in an Oxford Instruments liquid nitrogen cryostat. Just as for the transient absorption experiments, the UV−vis spectra of the samples were measured before and after the experiment in order to detect any photodecomposition.

The lifetimes of the emission were calculated by fitting the emission intensity measured at 20 different delay times after the laser excitation with the 100 ns gate to first-order kinetics. This was repeated for at least 20 different wavelengths, and the calculated lifetime was averaged. The emission quantum yields were measured relative to a standard solution of Re(Cl)(CO)$_3$(bpy) in 2-MeTHF ($\Phi_s = 0.028$ at 77 K),[13] using the 1 ms gate. Corrections were made according to eq 1,[44,45] in

$$\Phi_u = \Phi_s\left(\frac{I_u}{I_s}\right)\left(\frac{A_s}{A_u}\right) \quad (1)$$

which Φ is the emission quantum yield of the unknown (u) and standard (s) species, *I* the integrated emission intensity, and *A* the ground state absorbance at the wavelength of excitation (460 nm).

(33) Lumpkin, R. S.; Meyer, T. J. *J. Phys. Chem.* **1986**, *90*, 5307.
(34) Stor, G. J.; Stufkens, D. J.; Oskam, A. *Inorg. Chem.* **1992**, *31*, 1318.
(35) Rossenaar, B. D.; Stufkens, D. J.; Vlček, A., Jr. *Inorg. Chim. Acta*, in press.
(36) Stor, G. J.; Stufkens, D. J.; Vernooijs, P.; Baerends, E. J.; Fraanje, J.; Goubitz, K. *Inorg. Chem.* **1995**, *34*, 1588.
(37) Nieuwenhuis, H. A.; Stufkens, D. J.; Oskam, A. *Inorg. Chem.* **1994**, *33*, 3212.
(38) Nieuwenhuis, H. A.; Stufkens, D. J.; McNicholl, R.-A.; McGarvey, J. J.; Westwell, J.; George, M. W.; Turner, J. J. *J. Am. Chem. Soc.* **1995**, *117*, 5579.
(39) Nieuwenhuis, H. A.; Stufkens, D. J.; Vlček, A., Jr. *Inorg. Chem.* **1995**, *34*, 3879.
(40) Vogler, A.; Kunkely, H. *Comments Inorg. Chem.* **1990**, *9*, 201.
(41) Wang, Y.; Hauser, B. T.; Rooney, M. M.; Burton, R. D.; Schanze, K. S. *J. Am. Chem. Soc.* **1993**, *115*, 5675.
(42) Staal, L. H.; Oskam, A.; Vrieze, K. *J. Organomet. Chem.* **1979**, *170*, 235.
(43) Abel, E. W.; Wilkinson, G. *J. Chem. Soc.* **1959**, 1501.
(44) Parker, C. A.; Rees, W. T. *Analyst* **1962**, *87*, 83.
(45) Caspar, J. V.; Meyer, T. J. *J. Am. Chem. Soc.* **1983**, *105*, 5583.

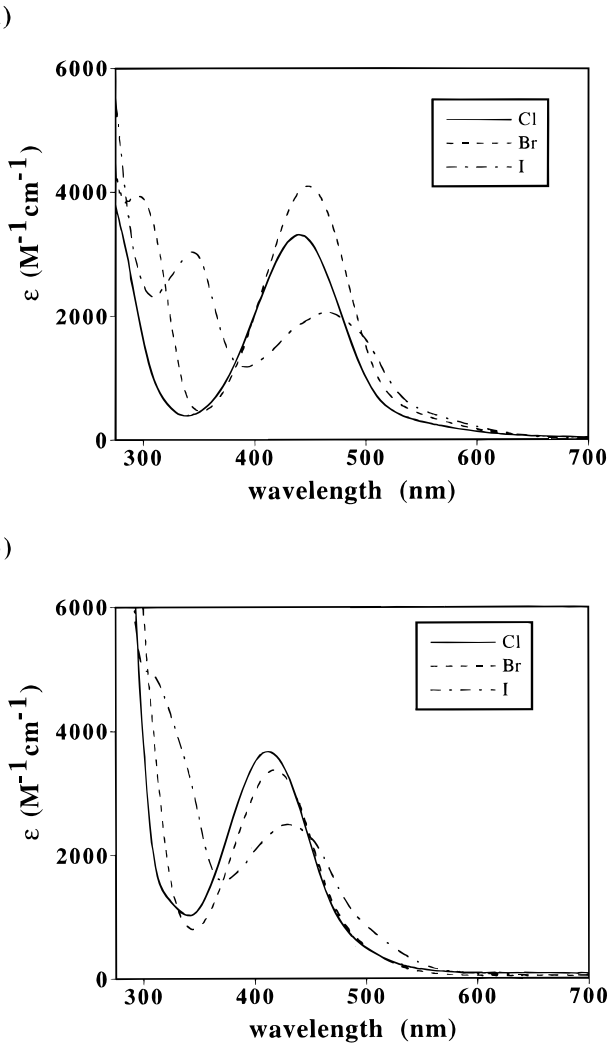

Figure 2. Electronic absorption spectra in THF at 293 K of (a) Re(X)(CO)$_3$(iPr-DAB) and (b) Re(X)(CO)$_3$(iPr-PyCa) (X = Cl, Br, I).

The rate constants for radiative (k_r) and nonradiative (k_{nr}) decay were calculated from eq 2.

$$\Phi = \frac{k_r}{k_r + k_{nr}} \qquad \tau = \frac{1}{k_r + k_{nr}} \tag{2}$$

Low-temperature excitation spectra were recorded on a Spex Fluorolog II emission spectrometer. The samples were dissolved in freshly distilled 2-MeTHF, freeze−pump−thaw degassed, and sealed under vacuum in a 1 cm cuvette. The concentration was such that the maximum absorption did not exceed 0.2.

Results and Discussion

In the following sections, the absorption and resonance Raman spectra, the emission at low temperatures, and the time-resolved absorption spectra of the complexes Re(X)(CO)$_3$(α-diimine) (X = halide) will be described and discussed. The abbreviation X/α-diimine will be used throughout this paper. It stands for Re(X)(CO)$_3$(α-diimine), *e.g.* Cl/iPr-DAB means Re(Cl)(CO)$_3$(iPr-DAB).

Absorption and Resonance Raman Spectra. The absorption spectra of the complexes X/iPr-DAB and X/iPr-PyCa in THF at room temperature are depicted in Figure 2. The absorption maxima and extinction coefficients are collected in Table 1, and the absorption data at low temperature are summarized in Table 2.

Table 1. Absorption Maxima[a] and Extinction Coefficients[b] (in Parentheses) of Re(X)(CO)$_3$(α-diimine) Complexes at Room Temperature

		X		
α-diimine	solvent	Cl	Br	I
iPr-DAB	THF	441 (3.3)	297 (sh); 448 (4.1)	344 (3.0); 465[c] (2.1)
	toluene	459	304 (sh); 466	357; 480[c]
iPr-PyCa	THF	411 (3.7)	286 (sh); 417 (3.4)	310 (5.1); 429[c] (2.5)
bpy	THF	389 (3.2)	392 (3.0)	∼320 (sh);403[c] (2.4)

[a] In nm. [b] In 10^3 M^{-1} cm^{-1}. [c] This absorption band is composed of three apparent maxima separated by *ca.* 1200 cm^{-1}.

Table 2. Emission Properties of Re(X)(CO)$_3$(α-diimine) Complexes (Abbreviated as X/α-diimine) in a 2-MeTHF glass (80 K)

compound	λ_{abs}[a]	λ_{em}[a]	ΔE_{abs-em}[b]	τ[c]	$10^4\Phi$	k_r[d]	$10^{-4}k_{nr}$[d]
Cl/iPr-DAB	402	668	9906	0.03	0.05	163	3570
Br/iPr-DAB	413	666	9198	0.06	0.12	200	1700
I/iPr-DAB	428[e]	658	8167	0.2	0.41	193	470
Cl/iPr-PyCa	394	605	8852	0.4	20	4843	242
Br/iPr-PyCa	396	600	8586	0.7	13	1823	138
I/iPr-PyCa	408[f]	590	7561	1.9	16	843	54
Cl/bpy	375	532	7870	2.7	280[g]	10370	36.0
Br/bpy	378	530	7587	3.7	488	13189	25.7
I/bpy	388[h]	525	6726	7.5	660	8800	12.5

[a] In nm. [b] In cm^{-1}. [c] In μs; estimated error ±10%. [d] In s^{-1}. [e] Three apparent maxima separated by 1090 cm^{-1}. [f] Three apparent maxima separated by 980 cm^{-1}. [g] From ref 13. [h] Three apparent maxima separated by 1325 cm^{-1}.

The absorption spectra of all complexes studied consist of two absorption bands in the 300−500 nm spectral region. Their position and intensity depend on the halide and α-diimine ligand used. In addition, intense bands, assigned to intraligand (IL) transitions of the α-diimine, are observed in the UV spectral region for the X/iPr-PyCa (<295 nm) and X/bpy complexes (<320 nm).

The intense lowest-energy absorption bands of the chloride and bromide complexes have similar integrated peak areas. They have been characterized earlier by different spectroscopic methods as originating in MLCT $d_\pi(Re) \rightarrow \pi^*$(α-diimine) transition(s).[1,11,46,47] For X = I, the peak area of this low-energy band is only ca. 60% of those of the Cl and Br complexes. In addition, this band becomes structured, giving rise to three apparent maxima separated by *ca.* 1200 cm^{-1} (see Figure 3c). The position of the main maximum depends very little on the halide X. This band shifts to higher energy upon cooling the solution to a glass (see Tables 1 and 3), due to the rigidochromic effect.[14] The magnitude of this effect is independent of the halide used. Furthermore, cooling results in a better resolved fine structure of the lowest-energy absorption band.

The second, higher-energy, absorption band shifts to lower energy upon going from Cl to Br to I. Whereas this band is very prominent for the iodo complexes (see Figure 2), it is concealed by the IL transitions in the case of the chloro complexes. For X = Br, this band is apparent as a shoulder for the iPr-DAB and iPr-PyCa complexes but obscured by the IL transitions for Br/bpy.

Changing the α-diimine ligand from bpy to iPr-PyCa to iPr-DAB results in all cases in a shift of the absorption maxima to longer wavelengths. This parallels the decreasing π^* energy of the α-diimine ligands,[47,48] indicating that the transitions are directed to the π^*(α-diimine) orbital. This charge transfer character is also evident from the negative solvatochromism of

(46) Kalyanasundaram, K. *J. Chem. Soc., Faraday Trans. 2* **1986**, *82*, 2401.
(47) Stufkens, D. J. *Coord. Chem. Rev.* **1990**, *104*, 39.
(48) Reinhold, J.; Benedix, R.; Birner, P.; Hennig, H. *Inorg. Chim. Acta* **1979**, *33*, 209.

Table 3. Resonantly Enhanced Raman Bands (cm^{-1}) of Re(X)(CO)$_3$(iPr-DAB) in KNO_3

X			
Cl	Br	I	assignt
2023	2020	2021	ν_s(CO)
1564	1555	1547	ν_s(CN)
1066			
633	628	632	
502	514	504	
485	500	487	
438	442	440	
	341		
283	189	154	ν(Re−X)

the two absorption bands. The magnitude of this solvent effect decreases going from Cl to Br to I.

In order to gain more insight into the character of the allowed electronic transitions, a resonance Raman (rR) study on X/iPr-DAB was carried out. (The strong luminescence of X/iPr-PyCa and X/bpy (*vide infra)* prevented the recording of good rR spectra of these complexes.) Table 3 presents the resonance-enhanced Raman bands of the X/iPr-DAB complexes obtained in a spinning KNO_3 pellet. These vibrations are assigned by analogy with those previously reported for Re(Cl)(CO)$_3$(iPr-DAB)[1] and with the spectra of other α-diimine−carbonyl complexes.[47] For all three complexes, the lower frequency bands, belonging to metal−ligand vibrations and ligand deformation modes, are rather weak compared with the CN stretching vibration. Figure 3 shows the rR excitation profiles for the two most strongly enhanced vibrations, ν_s(CO) and ν_s(CN). Since the rR spectra of I/iPr-DAB measured in a KNO_3 pellet were of rather poor quality, they had to be recorded in benzene for the excitation profiles (Figure 3c). Even then, these spectra could not be measured at longer excitation wavelengths at the low-energy side of the first absorption band due to disturbing emission. This makes a comparison of the excitation profiles of this complex with those of the Cl and Br complexes risky. The excitation profile of ν_s(CN) of the I complex is noteworthy since it shows a sharp decrease in intensity upon excitation into the second component of the absorption band. This may be caused by interference effects which have been observed previously in rR excitation profiles measured within composite absorption bands.[49]

The rR excitation profiles for the complexes Cl/iPr-DAB and Br/iPr-DAB show a weak rR effect for ν_s(CO) at *ca.* 2020 cm^{-1} and a much stronger effect for ν_s(CN) at *ca.* 1560 cm^{-1}. Both Raman bands show a gradual increase of intensity upon going to higher excitation energy, approaching the maximum of the absorption band. Although this behavior is typical for MLCT transitions,[47] there is still a difference between the intensity ratios of the ν_s(CO) and ν_s(CN) Raman bands of the two complexes. This ratio decreases from 0.22 to 0.13 going from the Cl to the Br complex.

A similar change in behavior upon going from Cl to I was recently found for the complexes Ru(X)(R)(CO)$_2$(α-diimine) (X = Cl, Br, I; R = alkyl).[37] This observation can be explained by a different extent of mixing of the metal d_π orbitals with the halide p_π orbitals. From Cl to Br and I, the p_π orbitals rise in energy, both absolutely (indicated by the ionization potentials of the halide p_π orbitals, as shown, *e.g.*, by a UV-PES study of M(X)(CO)$_5$ (M = Mn, Re; X = Cl, Br, I)[50,51]) and relative to the d_π(Re) orbitals. Thus, upon going from Cl to I, the lower-lying metal−halide π-bonding orbitals will obtain more metal character, while the corresponding π-antibonding orbital, which is the HOMO of the complex molecule, acquires more halide character (see Scheme 1). Thus, in the case of the bromo and iodo complexes, the lowest energy transitions will be more XLCT than MLCT in character. Recent SCF−MO calculations on *fac*-Mn(X)(CO)$_3$(bpy) (X = Cl, I)[36] have shown that substitution of Cl by I indeed results in an increase of halide character in the HOMO of the complex, which has 28% d_π(Mn) and 59% p_π(Cl) character for X = Cl and 11% d_π(Mn) and 83% p_π(I) character for X = I.

According to this proposed MLCT/XLCT change in character of the low-energy absorption band, its intensity decreases

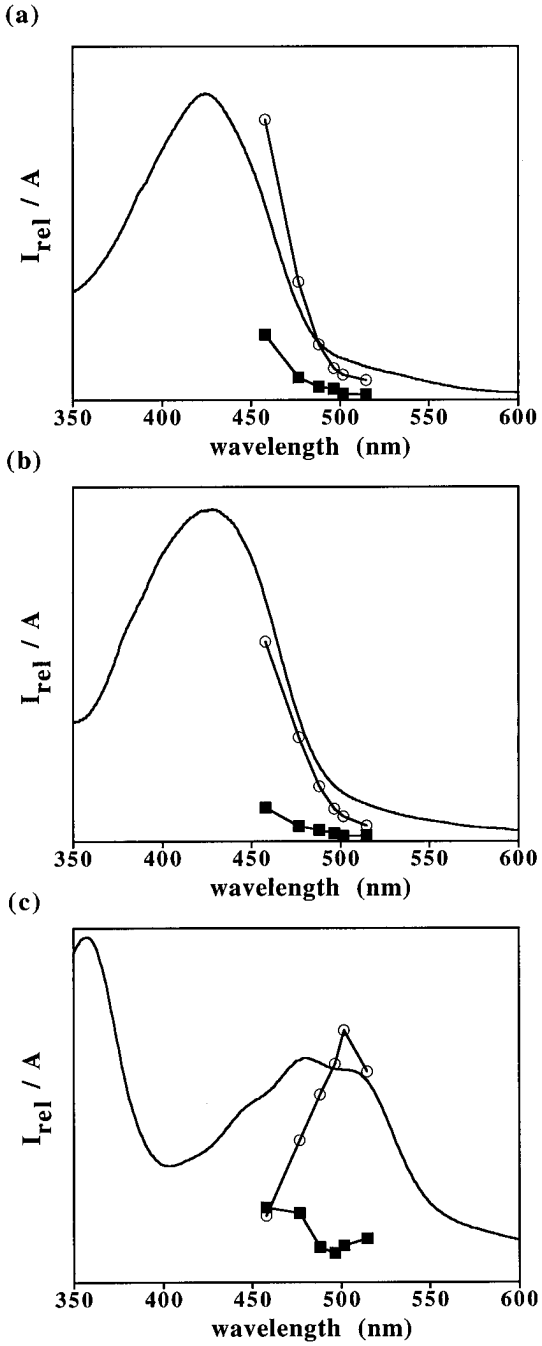

Figure 3. Resonance Raman excitation profiles of ν_s(CO) (■) and ν_s(CN) (○) for Re(X)(CO)$_3$(iPr-DAB): (a) X = Cl; (b) X = Br; (c) X = I. Intensities (I_{rel}) are relative to the 1050 cm^{-1} band of KNO_3 for (a) and (b). For (c) I_{rel} is relative to the 1178 cm^{-1} band of benzene. UV−vis absorption spectra were recorded in KBr for (a) and (b) and in benzene for (c).

(49) Clark, R. J. H.; Dines, T. J. *Angew. Chem., Int. Ed. Engl.* **1986**, *25*, 131.
(50) Higginson, B. R.; Lloyd, D. R.; Evans, S.; Orchard, A. F. *J. Chem. Soc., Faraday Trans. 2* **1975**, *71*, 1913.
(51) Jolly, W. L. *J. Phys. Chem.* **1983**, *87*, 26.

Scheme 1. Qualitative MO Scheme for $Re(X)(CO)_3(\alpha\text{-diimine})$[a]

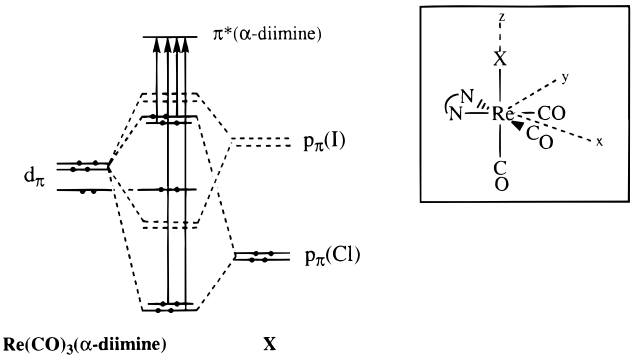

[a] The $d_\pi(Re)$ orbitals (d_{xz} and d_{yz}) of the $Re(CO)_3(\alpha\text{-diimine})$ unit interact with the $p_\pi(X)$ (p_x and p_y) orbitals, resulting in π-bonding ($d_\pi(Re) + p_\pi(X)$) and π-antibonding ($d_\pi(Re) - p_\pi(X)$) combinations. The $d_{xy}(Re)$ orbital is nonbonding with respect to the halide. The solid lines show the orbital diagram for X = Cl; the dashed lines, the situation for X = I.

substantially upon going from Cl to I (*vide supra*). This is caused by the much smaller overlap with the $\pi^*(\alpha\text{-diimine})$ orbital for the $p_\pi(X)$ orbitals than for the $d_\pi(Re)$ orbital. Hence, the intensity of the transition to $\pi^*(\alpha\text{-diimine})$ from $d_\pi(Re) - p_\pi(X)$ will mainly be determined by the contribution of $d_\pi(Re)$ to the HOMO, which decreases upon going from Cl to I (see Scheme 1).

The $\nu_s(CN)$ stretching frequency decreases in the order Cl > Br > I (see Table 3). This points to an increase of electron density on the α-diimine ligand upon going from Cl to I, in accordance with the increased π-donation from the halide and the concomitant increase of π-back-bonding to the iPr-DAB ligand.

The appearance of three apparent band maxima in the lowest-energy absorption band of I/α-diimine may be caused by a partly resolved vibronic structure. The separation between the apparent maxima, approximately 1200 cm^{-1}, suggests that it originates in the intraligand vibrations.

Since the position of the higher-energy absorption band of the I/iPr-DAB complex is outside the wavelength region of the laser lines, its character could not be determined by rR measurements. However, by analogy with $Ru(X)(R)(CO)_2(\alpha\text{-diimine})$, we tentatively assign this band to MLCT transition(s) from the π-bonding $d_\pi(Re) + p_\pi(X)$ orbitals to the $\pi^*(\alpha\text{-diimine})$ orbital (see Scheme 1). The increased intensity of this band with respect to those of the chloro and bromo complex is explained by the increased metal character in the metal−halide bonding combination.

Low-Temperature Emission. A qualitative comparison of the absorption, rR, and emission spectra is of interest here, since the same orbitals will be involved in the absorption and emission of these complexes. All complexes show a single unstructured emission band in a 2-MeTHF glass at 80 K (see Table 2). The difference in structure between the absorption and emission (see Figure 4) is not unexpected since absorption takes place to a triplet state (spin−orbit coupling).

Figure 4 shows the absorption, emission and excitation spectra of I/iPr-PyCa. The excitation spectrum measured by monitoring the emission at 590 nm matches perfectly the low-temperature absorption spectrum, indicating that the emitting state is efficiently populated from the optically excited state independently of the excitation wavelength.

Going from Cl to Br to I, the emission maximum shifts slightly to higher energy. The emission lifetime is mainly determined by the rate of the nonradiative decay, k_{nr}, which is

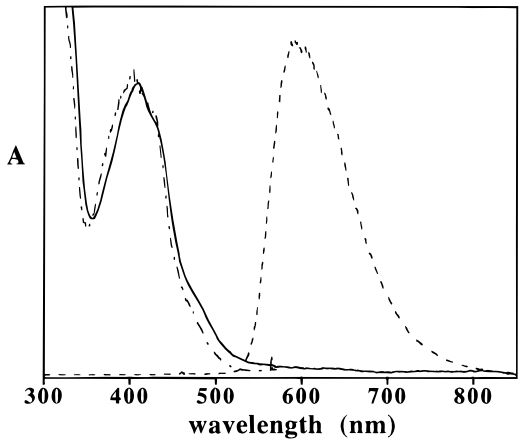

Figure 4. Ground state absorption (—), emission (- - -), and excitation (— • — •) spectra of I/iPr-PyCa in a 2-MeTHF glass at 80 K.

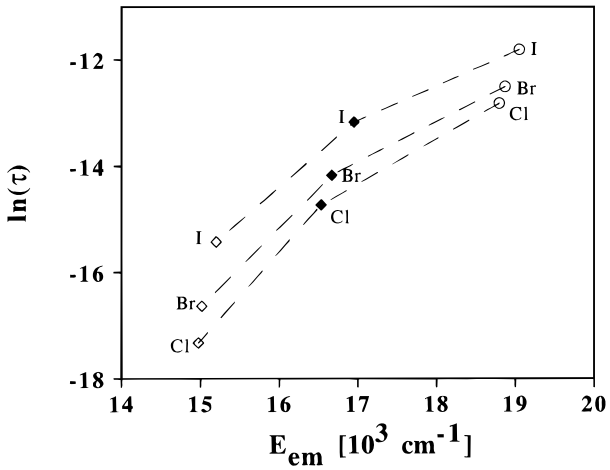

Figure 5. Plot of $\ln(\tau)$ (τ in s) *vs* E_{em} for the emission of $Re(X)(CO)_3(\alpha\text{-diimine})$ in a 2-MeTHF glass (80 K): ○ = X/bpy; ◆ = X/iPr-PyCa; ◇ = X/iPr-DAB.

1 to 5 orders of magnitude higher than the radiative decay rate, k_r, depending on X and the α-diimine used.

The influence of the ligands X and α-diimine on the nonradiative decay rate and, thus, on the excited state lifetime (τ) may be discussed using Figure 5, which shows a plot of $\ln(\tau)$ *vs* the emission energy. It is obvious that the X/α-diimine complexes do not behave as a homogeneous class of compounds whose emission simply follows the energy gap law.[2,32,33,52] For each particular α-diimine ligand, the excited state lifetime sharply increases in the order Cl < Br < I, whereas the emission energy hardly changes. The emission lifetimes thus clearly point to a change in character of the emitting excited state from MLCT for X = Cl to XLCT for X = I, in accordance with the evidence obtained from the absorption and rR spectra (*vide supra*). The apparent Stokes shift, ΔE_{abs-em} (see Table 2), significantly decreases in the order Cl > Br > I. This indicates a smaller excited state distortion in the XLCT than MLCT excited states that appears to be responsible for the larger XLCT lifetimes. Such an effect was found also for $Ru(X)(R)(CO)_2(\alpha\text{-diimine})$ complexes.[39]

The rate of the nonradiative decay, k_{nr}, and, hence, the excited state lifetime are very dependent on the α-diimine. Figure 5 shows that the lifetime decreases in the order bpy > iPr-PyCa > iPr-DAB. This correlates with the decreasing emission

(52) Kober, E. M.; Caspar, J. V.; Lumpkin, R. S.; Meyer, T. J. *Inorg. Chem.* **1986**, *90*, 3722.

energy and may, essentially, be accounted for by energy gap law effects. At the same time, the apparent Stokes shift increases significantly in the order bpy < iPr-PyCa < iPr-DAB. This suggests a parallel rise in the excited state distortion, which also contributes to the rate of the nonradiative excited state deactivation. This order basically reflects the increasing Re → α-diimine π-back-donation.[47] Due to the increasing mixing of the d_π(Re) and π^*(α-diimine) orbitals, the low-frequency skeletal vibrations can effectively contribute to the nonradiative deactivation of the MLCT or XLCT excited states of PyCa and, especially, DAB complexes. Also the increased flexibility of the DAB ligand may provide efficient nonradiative deactivation pathways. This dependence on the α-diimine is not restricted to these $Re(X)(CO)_3$(α-diimine) complexes; the same trend was observed, *e.g.*, for $Ru(X)(R)(CO)_2$(α-diimine)[39] and $W(CO)_4$-(α-diimine).[53,54] The extensive delocalization within the Re-(iPr-DAB) chelate ring may also explain the larger-than-expected lifetime drop between iPr-Pyca and iPr-DAB complexes (see Figure 5).

The sensitivity of k_{nr} to the α-diimine decreases upon going from Cl to Br to I. For the chloro complexes, variation of the α-diimine from bpy to iPr-PyCa or iPr-DAB results in an increase of k_{nr} by a factor of 6.7 or 99, respectively. For the bromo and iodo complexes these factors are 5.4, 66 and 4.3, 38, respectively. This effect reflects the changing mechanism of excited state deactivation for these complexes upon variation of X. The MLCT excited state of the chloro complexes is mainly deactivated via vibrations of the bonds of the Re(α-diimine) ring, because of a relatively large distortion of this chelate ring caused by depopulation of the Re−N π-bonding (essentially d_π) and population of Re−N π-antibonding (essentially α-diimine π^*) orbitals. Since the Re−N π-bonding orbital is not depopulated for the iodo complexes, this deactivation pathway becomes much less important. This is experimentally manifested by the overall increase of the excited state lifetime and decrease of the apparent Stokes shift.

In conclusion, all the trends in the excited state dynamics coherently point to the gradual change of character of the lowest (emitting) excited state as a function of X, which parallels the information obtained from the UV−vis and resonance Raman spectra (*vide supra*). This also points to a difference in lowest-excited-state character between Br/α-diimine and Cl/α-diimine, which was never realized before. For, both Cl/bpy and Br/bpy have always been regarded as emitting from an MLCT excited state.[28]

Not only does the rate of nonradiative decay depend on the α-diimine, but a similar trend is observed for the radiative decay rate, which decreases in the order bpy >> iPr-PyCa > iPr-DAB. The dependence on the halide is not regular, but a higher value of k_r is generally obtained for the MLCT state than for the XLCT state. The values of k_r of I/α-diimine complexes, in comparison with Cl/α-diimine, are significantly lower (iPr-PyCa, bpy) or similar (iPr-DAB) in accordance with the changed excited state character. The decrease of the radiative deactivation upon going from the MLCT excited state to the XLCT state again reflects the partial overlap-forbiddeness of the XLCT → ground state transition. This is in full agreement with the smaller extinction coefficients of the XLCT absorption bands of the I/α-diimine complexes, as compared with their chloro and bromo counterparts. The combination of a relatively high k_r and low k_{nr} value for I/bpy makes this complex strongly emissive ($\Phi = 0.07$).

At room temperature in a THF solution, the excited state lifetimes of the X/iPr-PyCa and X/iPr-DAB complexes are too short (<20 ns) to be measured accurately. Only for the X/bpy complexes could reliable emission lifetimes be obtained, which are collected, together with the time-resolved absorption data, in Table 4. As in the low-temperature glass, the solution excited state lifetimes increase in the order Cl < Br ≪ I.

Time-Resolved Absorption Spectroscopy. In order to gain more insight into the excited state character of the complexes $Re(X)(CO)_3$(α-diimine) in fluid solution as a function of the halide X, time-resolved absorption spectra of these complexes were measured in THF solution at room temperature. Unfortunately, the lifetimes of the excited state of the complexes X/iPr-DAB and X/iPr-PyCa were too short (*vide supra*) to measure the excited state absorptions accurately. However, the lifetimes of the excited states of the X/bpy complexes appeared to be long enough and reliable excited state spectra were obtained.

Figure 6 presents the ground state absorption spectra of X/bpy (X = Cl, Br, I) together with their transient absorption spectra obtained 10 ns after 460 nm excitation. The latter spectra are corrected for emission of the complex due to the laser excitation. In Table 4 the lifetimes and absorption maxima of the transients are summarized. The similarity of the emission lifetimes and those calculated from the decay of the transient absorption suggests that the emission and transient absorption originate from the same excited state.

The spectral pattern found for the excited state of Cl/bpy is very similar to that reported earlier for Cl/bpy in acetonitrile[46] and also comparable to the one reported by us for Br/bpy′ in THF.[35] The transient absorption spectra were in both cases assigned to the ^{3}MLCT state, supported by the evidence from time-resolved Raman[11] and IR spectroscopies.[4,27,55] The two bands at 375 and 470 nm present in the transient spectra of all three X/bpy complexes can be attributed to the $\pi_1^* \rightarrow \pi_2^*$ and $\pi \rightarrow \pi_1^*$ IL transitions of the $(bpy)^{\cdot -}$ chromophore present in the excited molecules, since they closely resemble the bands found in the absorption spectrum of reduced $[bpy]^{\cdot -}$ generated independently.[56,57] Also the absorption spectrum of reduced $[Re(Br)(CO)_3(bpy')]^-$, with the extra electron localized on the bpy′ ligand, possesses bands in this region with comparable shape and relative intensity.[35]

In addition, a third, hitherto unrecognized, band was detected in the spectra, whose position and intensity depend strongly on the halide X. This band was observed as a weak shoulder at *ca.* 510 nm for X = Cl, at *ca.* 590 nm for X = Br, and at 780 nm for X = I (see Figure 6). The intensity of this absorption band increases in the same order. The large influence of the halide on this absorption band renders its assignment to a $[bpy]^{\cdot -}$ intraligand transition rather improbable since no such halide effect was observed for the genuine IL transitions at 375 and 470 nm (*vide supra*). In order to determine whether the presence of an I^- ligand gives rise to such a transition, I/bpy was spectroelectrochemically reduced in nPrCN at 198 K. The absorption spectrum of the thus obtained $[I/bpy]^-$ showed an intense band at 365 nm, sharp bands at 475 and 500 nm, and a very weak absorption at 820 nm, which can all be assigned to an IL transition on the $[bpy]^-$ chromophore.[56,57] No intense absorption was observed in the 780 nm region.

(53) Manuta, D. M.; Lees, A. J. *Inorg. Chem.* **1983**, *22*, 572.
(54) Servaas, P. C.; van Dijk, H. K.; Snoeck, T. L.; Stufkens, D. J.; Oskam, A. *Inorg. Chem.* **1985**, *24*, 4494.
(55) Gamelin, D. R.; George, M. W.; Glyn, P.; Grevels, F.-W.; Johnson, F. P. A.; Klotzbücher, W.; Morrison, S. L.; Russell, G.; Schaffner, K.; Turner, J. J. *Inorg. Chem.* **1994**, *33*, 3246.
(56) Krejcík, M.; Vlček, A. A. *J. Electroanal. Chem. Interfacial Electrochem.* **1991**, *313*, 243.
(57) Noble, B. C.; Peacock, R. B. *Spectrochim. Acta* **1990**, *46A*, 407.

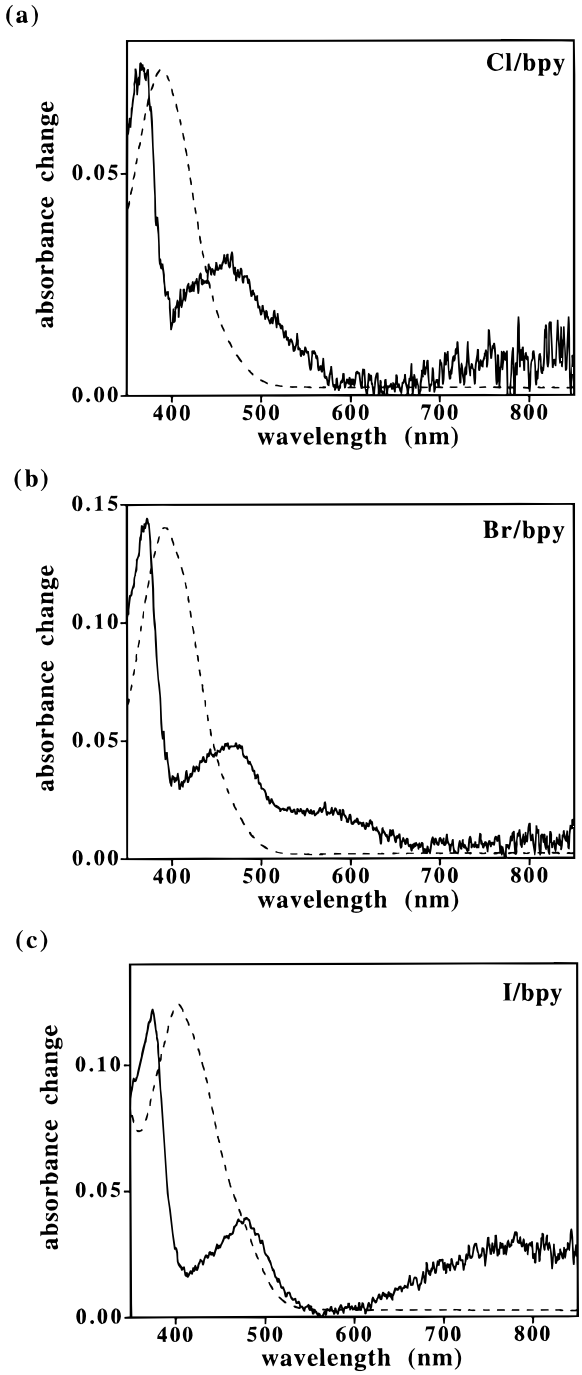

Figure 6. Ground state (- - -) and transient absorption (—) spectra of $Re(X)(CO)_3(bpy)$ in THF measured 10 ns after laser excitation at 460 nm: (a) X = Cl; (b) X = Br; (c) X = I.

Table 4. Transient Absorption and Emission Maxima (nm) and Excited State Lifetimes (ns) of $Re(X)(CO)_3(bpy)$ in THF at Room Temperature

complex	λ_{max}(TA)	τ(TA)[a]	λ_{max}(em)	τ(em)[a]
Cl/bpy	375, 470, 510	50	612	45
Br/bpy	375, 470, 590	57	605	55
I/bpy	375, 470, 780	95	601	79

[a] Estimated error ±10%.

We tentatively assign this third absorption to a transition from the Re−X π-bonding $d_\pi(Re) + p_\pi(X)$ orbital to the corresponding antibonding $d_\pi(Re) - p_\pi(X)$ orbital. For X = Cl, this transition is directed from a mainly halide-based orbital to a metal orbital, *i.e.* a transition from the MLCT excited state to the XLCT excited state. For X = Br, the transition is delocalized over the halide and metal, a $(d_\pi + p_\pi) \rightarrow (d_\pi - p_\pi)$ transition. The transient absorption of the iodo complex is assigned to a transition from the XLCT state to the MLCT state (see Scheme 2). The red shift of this absorption band reflects a decreased splitting of the bonding and antibonding metal−halide orbitals upon going from Cl to I, which was found also in the ground state absorption spectra of I/iPr-DAB. For I/iPr-DAB, a splitting of 7560 cm^{-1} is estimated from the difference between the two ground state absorption maxima; for X = Br it is 11 350 cm^{-1}, and for X = Cl a lower limit of 14 360 cm^{-1} is derived. Unfortunately, these splitting values could not be calculated for X/bpy, since the higher energy transitions are obscured by the intense IL absorptions in the UV spectral region. Although direct comparison of these values with the observed transition energies estimated from the transient absorption spectra is impossible due to different contributions from electron correlations, the observed trend is quite comparable with the shift to lower energy of the transient absorption maximum upon going from Cl to Br to I (~19 610, 16 950, and 12 820 cm^{-1}, respectively).

Scheme 2. Qualitative MO Scheme for $Re(Cl)(CO)_3(\alpha\text{-diimine})$ (Left) and $Re(I)(CO)_3(\alpha\text{-diimine})$ (Right) in the CT Excited State[a]

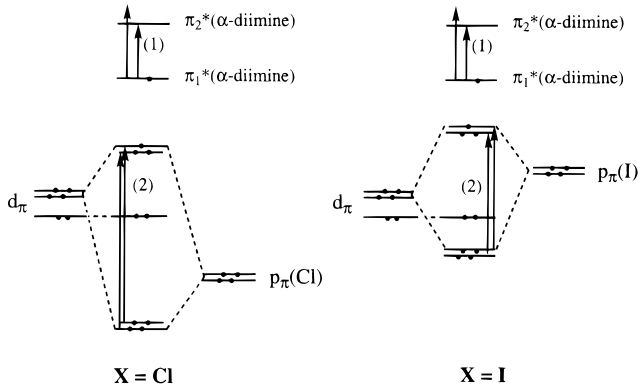

[a] Key: (1) $\pi_1^* \rightarrow \pi_2^*$ IL transition; (2) transition between bonding and antibonding metal−halide orbitals, probably responsible for the lowest energy absorption band in the time-resolved absorption spectrum.

The halide ligand clearly has a profound influence on all the excited state characteristics of the X/α-diimine complexes, which may be accounted for by a changing character of the lowest excited state from MLCT (X = Cl) to XLCT (X = I). The Br/α-diimine complexes are an intermediate case; their behavior, however, indicates a dominant MLCT character. Thus, both the solution and the low-temperature lifetimes increase only slightly upon going from Cl to Br, followed by a much more prominent rise observed for the iodo complexes. Also the ground state absorption spectra and the rR excitation profiles of X/iPr-DAB are alike for X = Cl and Br, but completely different for X = I. Finally, the changed excited state character is, for I/bpy, evidenced by the appearance of a rather prominent excited state absorption band at relatively low energy. This band cannot be attributed to an intraligand transition. It appears to be characteristic of the XLCT excited state. A similar influence of X on the excited state absorption spectrum was recently reported for the complexes $Ru(X)(Me)(CO)_2$(iPr-DAB).[38] In that case, the transient absorption spectra exhibited bands at 420 nm for X = Cl (τ = 50 ns), at 450 nm with a shoulder at ~530 nm for X = Br (τ = 70 ns), and at 400 and 590 nm for X = I (τ = 180 ns). The origin of this effect of the halide ligand on the excited state may be similar for both classes of complexes.

Conclusions

The character of the excited state of the $Re(X)(CO)_3(\alpha\text{-diimine})$ complexes depends strongly on the halide X. For X = Cl, the lowest excited state could be characterized as MLCT while upon changing the halide to Br^- and, especially, to I^-, the lowest excited state gains more halide character and can be described as originating from an $X \rightarrow \pi^*(\alpha\text{-diimine})$ XLCT excitation. This influence of X is attributed to the halide-dependent extent of mixing of the $d_\pi(Re)$ and $p_\pi(X)$ orbitals, which increases with increasing $p_\pi(X)$ orbital energy.

Compared with the MLCT excited state, the XLCT excited state is characterized by a longer lifetime, due to a slower nonradiative decay to the ground state. The XLCT state is also a better luminophore because of the higher emission quantum yields. Variation of the α-diimine determines the lifetime of the excited states by affecting both the emission energy and k_{nr}. The MLCT state is more sensitive to those changes of the α-diimine than the XLCT state.

This study has shown that the character and dynamics of the lowest excited state of $Re(X)(CO)_3(\alpha\text{-diimine})$ complexes can be finely tuned by variation of the halide and α-diimine ligands.

Acknowledgment. The Netherlands Foundation for Chemical Research (SON) and the Netherlands Organization for Pure Research (NWO) are thanked for financial support. Partial support from the Granting Agency of the Czech Republic (Grant 203/93/0250) and from the European Scientific Network and COST Programs is also acknowledged.

IC9509802